

Short Communication

## Synthesis and the Electrochemical Performance of LiFePO<sub>4</sub>/C Cathode by Glucose-Assisted Carbothermal Reduction Method

Lei He, Puheng Yang, Shichao Zhang\*, Xin Wei, Guanrao Liu

School of Materials Science and Engineering, Beihang University, Beijing 100191, PR China

\*E-mail: [csc@buaa.edu.cn](mailto:csc@buaa.edu.cn)

Received: 26 January 2013 / Accepted: 25 March 2013 / Published: 1 May 2013

---

LiFePO<sub>4</sub>/C composites of high purity were synthesized by a carbothermal reduction method (CTR) using industrial raw materials and glucose as both reductive agent and carbon source. A required amount of ethanol was added to the starting materials for a ball milling process and the precursor was sintered at 650 °C for 8 h to form crystalline phase LiFePO<sub>4</sub>/C. The structure and morphology of LiFePO<sub>4</sub>/C composite samples were characterized by X-ray diffraction, field-emissions scanning electron microscopy and transmission electron microscopy, and their electrochemical properties were investigated by charge–discharge tests. The results show that the LiFePO<sub>4</sub>/C cathode materials deliver an initial discharge capacity of 142.6 mAh·g<sup>-1</sup> at a 0.1C-rate between 4.2 and 2.5 V (vs. Li<sup>+</sup>/Li), and almost no capacity loss is observed even up to 20 cycles. Furthermore, the effect of pH value of the precursor was investigated by adapting 1 to 6. The particle size of the LiFePO<sub>4</sub>/C composite scales down with the increasing of the pH value of the precursor.

---

**Keywords:** LiFePO<sub>4</sub>/C; cathode materials; carbothermal reduction method; lithium-ion battery.

### 1. INTRODUCTION

Olivine-structured lithium iron phosphate (LiFePO<sub>4</sub>) proposed by Goodenough et al. is a popular cathode material because of its low toxicity, remarkable thermal stability, low raw materials' cost, and a relatively high theoretical specific capacity of 170 mAh·g<sup>-1</sup> with a discharge voltage plateau of 3.5 V versus Li/Li<sup>+</sup> [1–3]. However, its poor rate capability restricts the commercial application of LiFePO<sub>4</sub>, which attributes to low electronic conductivity (~10<sup>-9</sup> S cm<sup>-1</sup>) and slow diffusion of lithium ions across the two-phase boundary [2,4]. To overcome the drawbacks, tremendous efforts have been made to enhance the electronic and ionic conductivity of LiFePO<sub>4</sub> particles through various material processing approaches, such as carbon coating [5–7], metal-ion

doping [8–11], and reducing particle size [12–14]. Especially, utilizing carbon-coating and smaller particle sizes at the same time have been attempted to overcome these drawbacks of  $\text{LiFePO}_4$ , because a smaller particle size could shorten the diffusion length of the Li-ion, while carbon-coating would increase surface electronic conductivity [15].

Up to now, various synthesis methods have been developed to prepare  $\text{LiFePO}_4$  materials, including solid-state reactions [1,15], the sol–gel process [7,16], hydrothermal synthesis [17], microwave synthesis [18], the solvothermal method [19], mechanical activation [20,21], coprecipitation [22,23] and hard-templating approaches [24]. Unfortunately, the above methods are expensive because they either involve complicated steps or using expensive divalent iron compounds, such as  $\text{FeC}_2\text{O}_4 \cdot \text{H}_2\text{O}$ , as the starting material.

In this study, a series of  $\text{LiFePO}_4/\text{C}$  composites were synthesized by a simple and low-cost carbothermal reduction method. Herein, glucose was introduced as the carbon source and reductant, and choosing industrial raw materials of ferric nitrate, ammonium dihydrogen phosphate, and lithium nitrate as starting materials, lower cost than other similar materials. The structure, morphology, electrochemical properties of  $\text{LiFePO}_4/\text{C}$  composites were investigated by using X-ray diffraction (XRD), scanning electron microscopy (SEM), transmission electron microscopy (TEM), and charge-discharge test. It is also investigated that the effect of the electrochemical performance of the samples with the increasing of pH value in the solution for preparation of precursors.

## 2. EXPERIMENTAL

A certain amount of  $\text{Fe}(\text{NO}_3)_3 \cdot 9\text{H}_2\text{O}$  was added to 0.6 M citric acid solution under the constant stirring, and then the mixture was aged at 60 °C for half an hour. Afterwards,  $\text{LiNO}_3$  (0.1M),  $\text{NH}_4\text{H}_2\text{PO}_4$  (0.1M) were added to the as-prepared mixture. HCl or  $\text{NH}_4\text{OH}$  was added to control the pH of the precursor solution. The pH of the precursor solution was adjusted from 1 to 6 by adding HCl/ $\text{NH}_4\text{OH}$  (denoted as pH1, pH2, pH3, pH4, pH5, pH6). The obtained mixture was stirred at 80 °C at least 5 h. After evaporating the water, the gel was obtained, and dried at 80 °C for 5 h. Following that, the gel precursor was grounded and then calcined at 400 °C for 4 h in  $\text{N}_2$  atmosphere. To coat  $\text{LiFePO}_4$  with carbon, glucose (45 wt.% of the gel precursor) was added to the above powder and mixed by ball-milling in the required amount of ethanol for 6h. The resulting mixture was dried at 60 °C in a vacuum oven and thoroughly reground. Finally, the dried mixture was transferred to a temperature controlled tube furnace equipped with flowing  $\text{N}_2$  gas and sintered at 650 °C for 8 h.

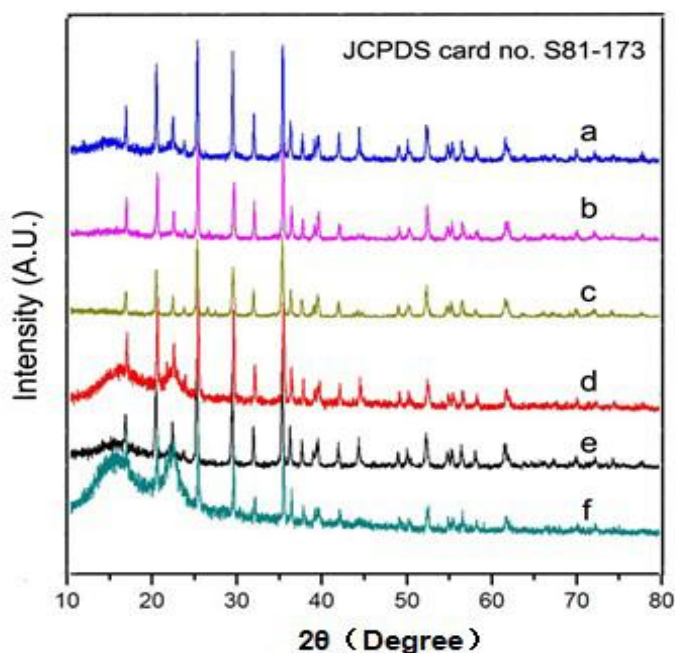
Crystal structural analysis of the CTR synthesized materials was carried out by X-ray diffraction (XRD, Rigaku D/Max-2400) with Cu  $K\alpha$  radiation. The diffraction patterns were recorded between scattering angles of 10° and 80° with the scanning rate of 6 °/min. The morphology of  $\text{LiFePO}_4/\text{C}$  composite was observed by scanning electron microscopy (SEM, Hitachi S- 4800), and transmission electron microscopy (TEM, JEOL JEM 2100F). The carbon distribution was confirmed with energy dispersive spectroscopy (EDS).

The testing half-cells of both kinds of electrodes were assembled in an Ar filled glove box (MB-10-G with TP170b/mono, MBRAUN) with a lithium sheet as a counter and reference electrode.

Electrolyte was 1M  $\text{LiPF}_6$  in a mixed solution of EC and DEC (1:1 in volume ratio). The materials were pressed into a thin film (75 wt% of the active material, 10 wt% of polyvinylidene fluoride (PVDF) in N-methyl pyrrolidone (NMP) and 15 wt% carbon black). The film was cut into pieces of about  $0.8 \times 0.8 \text{ cm}^2$  to act as electrodes and then dried at  $60 \text{ }^\circ\text{C}$  for 10h in a vacuum oven. The charge-discharge measurements were galvanostatically carried out in a battery test system (NEWARE BTS-610, Newware Technology Co., Ltd., China) at a constant current density, with cut off voltage of 2.5-4.2V (vs.  $\text{Li/Li}^+$ ).

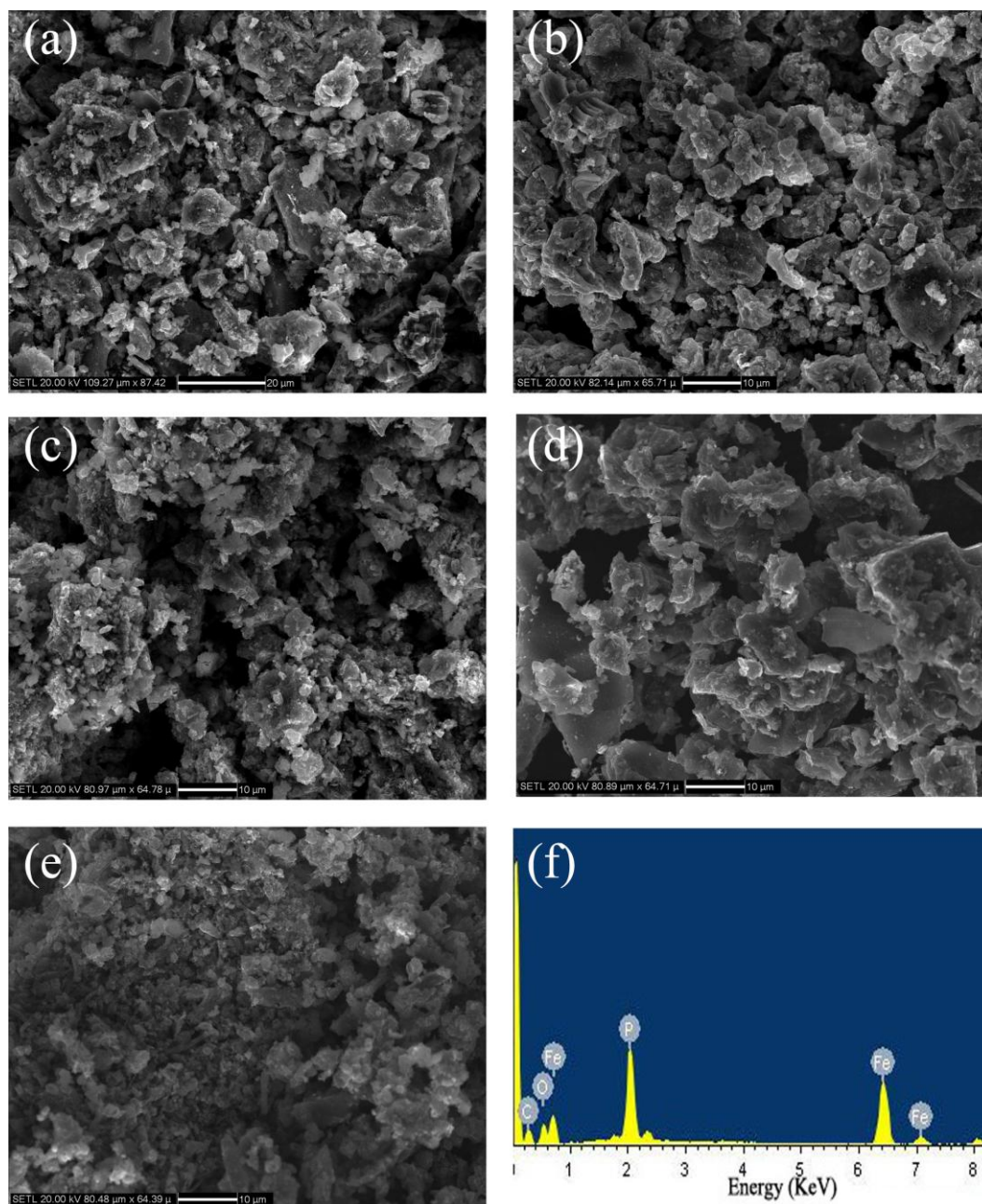
### 3. RESULTS AND DISCUSSION

The typical XRD patterns of the as-prepared  $\text{LiFePO}_4/\text{C}$  samples, which were prepared from the precursor solution with pH value varying from 1 to 6, are showed in Fig. 1. The diffraction peaks of all the samples are identified as those of the orthorhombic structure with the space group Pnma without any secondary phases such as  $\text{Fe}_2\text{P}$  and  $\text{Fe}_3\text{P}$ , suggesting that the carbon derived from the glucose can effectively avoid the appearance of the impurity phase during the CTR. The diffraction data are indexed to the orthorhombic Pnma space group (JCPDS card no. S81-1173). The lattice parameters of all  $\text{LiFePO}_4/\text{C}$  composite samples show good agreement with those of  $\text{LiFePO}_4$ . It is indicated that the pH value of the precursor has no marked effect on the structure of  $\text{LiFePO}_4$  materials. The results obtained from EDS show that the amount of carbon in the  $\text{LiFePO}_4/\text{C}$  composite are 25wt%. But there is no obvious diffraction response of the carbon because of its amorphous state. Similar results have been reported by Liu et al [25].



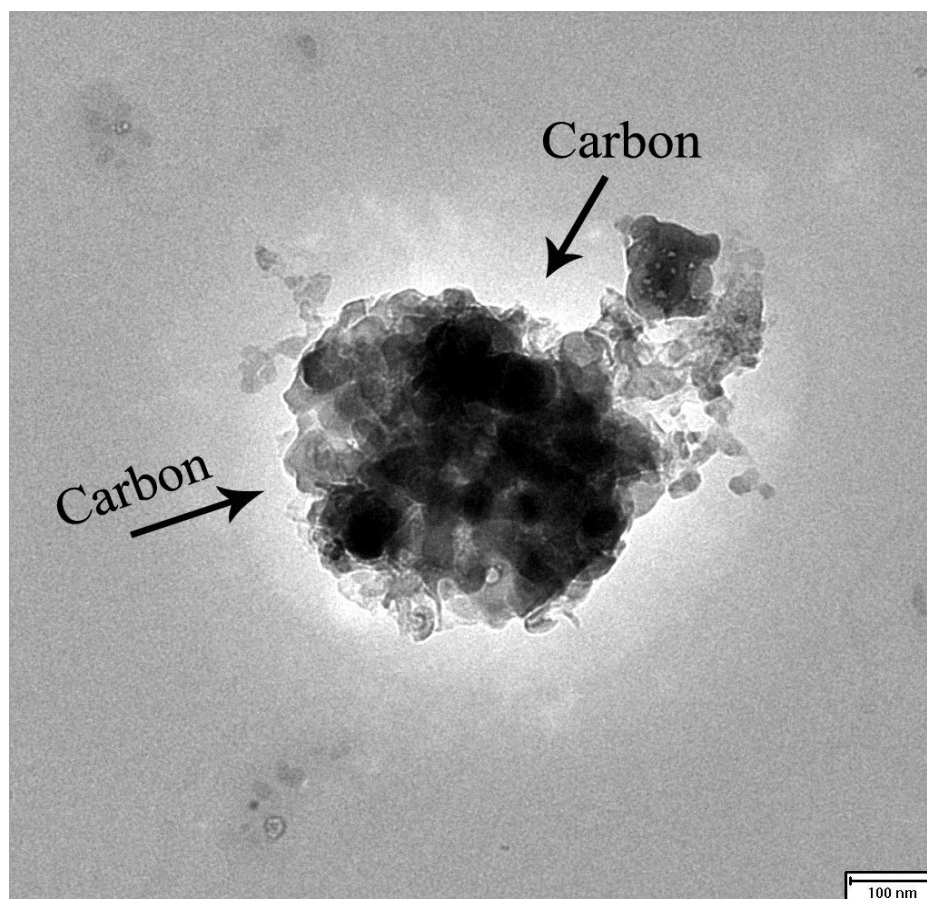
**Figure 1.** XRD patterns of the  $\text{LiFePO}_4/\text{C}$  composite samples prepared by glucose-assisted carbothermal reduction (CTR) method with various pH value of the precursor. (a)pH1; (b)pH2; (c)pH3; (d)pH4; (e)pH5; (f)pH6.

Fig. 2 shows the SEM image of the synthesized  $\text{LiFePO}_4/\text{C}$  particles under different pH conditions. By controlling pH value, an interesting morphological change of  $\text{LiFePO}_4/\text{C}$  composite can be observed. When the pH value is increased to 6, the particle is uniformly distributed and much smaller than the others, which maybe contribute to improve the electrochemical properties of the sample. Moreover, as a powder with such small particles has a large specific surface area, the conclusion was drawn that this suitability for the convenient movement of lithium ions should enhance electrochemical performance [26].



**Figure 2.** SEM images of the  $\text{LiFePO}_4/\text{C}$  samples obtained with different pH value: (a)pH2; (b)pH3;(c)pH4; (d)pH5; (e)pH6; (f) are the element analyses in sample (e) by EDS.

The particle size and the carbon morphology can be observed in TEM images. The  $\text{LiFePO}_4/\text{C}$  composite with pH 6 is composed of a mounts of sphere-like shape nanocrystals, with the size ranging from 100 to 300 nm as shown in Fig. 3. It is obvious that the carbon webs formed from the decomposition of glucose are wrapping and connecting the  $\text{LiFePO}_4$  particles, and thus prevented the further growth of  $\text{LiFePO}_4$  particles during high-temperature sintering. The presence of carbon webs plays an important role in inhibiting the growth of  $\text{LiFePO}_4$  particles and improving the electronic conductivities of materials.



**Figure 3.** Typical TEM image of the pH6 sample.

Fig. 4 presents the charge–discharge curves of the prepared materials at different pH value at a rate of 0.1C. The prepared material delivered a discharge capacity of 67.8, 78.4, 101.2, 107.0, 111.7, 113.7 and 142.6  $\text{mAh}\cdot\text{g}^{-1}$  at various pH value from 1 to 6, respectively. It is suggested that lower pH value might lead to poorer crystalline  $\text{LiFePO}_4/\text{C}$  and, higher pH value might result in smaller particle sizes, which are consistent well with the results in Fig. 2. Thus, it is important to find the optimum pH value of the precursor for  $\text{LiFePO}_4/\text{C}$ . As shown the charge–discharge curves of the material at pH6 in Fig. 4, the appearance of well-defined voltage plateaus at approximately 3.5 and 3.3V on the charge and discharge curves reflect the typical characteristics of olivine  $\text{LiFePO}_4$  [27].



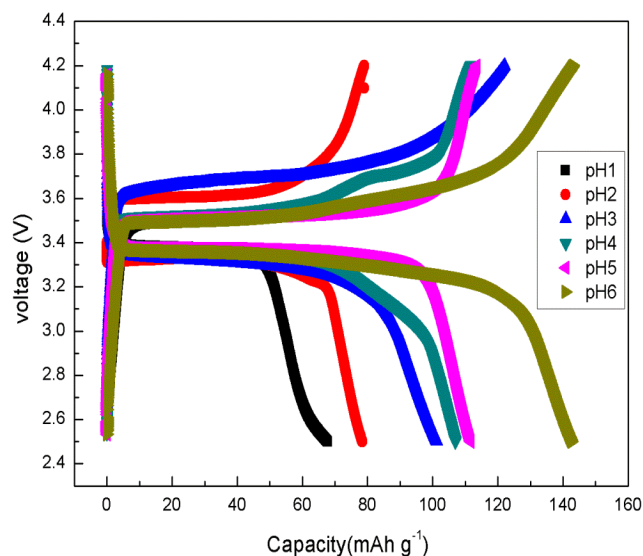


**Figure 4.** The charge/discharge profiles of the in the voltage from 2.5 to 4.2 V under various pH conditions.

Fig. 5 shows the cycling performance of  $\text{LiFePO}_4/\text{C}$  with different pH value at 0.1C. Obvious capacity decreased is observed at pH1 and pH2 after 10 cycles. However, the charge retention of the other  $\text{LiFePO}_4/\text{C}$  at 0.1C rate was 100%, indicating that most of the capacity in the composite can be released in high pH value. The good cycling behavior is mainly attributed to the nanometric particle size and enhancement of the electronic conductivity by the uniform carbon coating [28]. Notably, this  $\text{LiFePO}_4/\text{C}$  composite at pH6 exhibited excellent rate capability (Fig. 4) and remains  $135 \text{ mAh}\cdot\text{g}^{-1}$  at the 20<sup>th</sup> cycle.

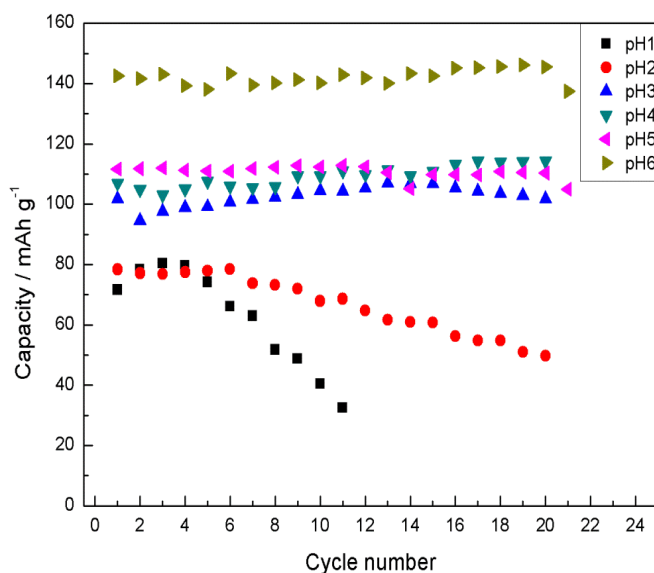


**Figure 5.** Cycle performance of all the  $\text{LiFePO}_4/\text{C}$  electrodes at 0.1C rate.

#### 4. CONCLUSIONS

Olivine  $\text{LiFePO}_4/\text{C}$  had been synthesized successfully at different pH conditions via a carbothermal reduction method using glucose as both carbon source and reducing agent. In the adapting pH process, it was found that pH value play multifold roles in controlling the morphology of  $\text{LiFePO}_4/\text{C}$  particles. The material synthesized at pH6 by glucose-assisted CTR owned the sphere-like shape nanocrystals with the size ranging from 100 to 300 nm, has a best electrochemical performance and its discharge capacity is about  $143 \text{ mAh}\cdot\text{g}^{-1}$  at 0.1C rate with satisfactory capacity retention. These improved electrochemical performances can be attributed to the unique microstructure, smaller size of the particle and the presence of carbon webs, which is favorable for increasing the electrochemical reaction surface, enhancing the electronic conductivity, and promoting lithium ion diffusion. On a general point, we believe the low-cost starting materials and excellent electrochemical performance are meaningful for application and commercialization as cathode materials of lithium-ion battery.

#### ACKNOWLEDGEMENTS

This work was supported by the National Basic Research Program of China (973 Program) (2013CB934001), National Natural Science Foundation of China (51074011 and 51274017) and National 863 Program (2007AA03Z231 and 2011AA11A257).

#### References

1. A.K. Padhi, K.S. Nanjundaswamy, J.B. Goodenough, *J. Electrochem. Soc.* 4 (1997) 144.
2. A.S. Andersson, J.O. Thomas, *J. Power Sources* 97–98 (2001) 498.
3. S. Scaccia, M. Carewska, P. Wisniewski, P. P. Prosini, *Mater. Res. Bull.* 7 (2003) 38.
4. P.P. Prosini, M. Lisi, S. Scaccia, *J. Electrochem. Soc.* 3 (2002) 149.
5. N. Ravet, J.B. Goodenough, S. Besner, P. Simoneau, M. Hovington, M. Armand, *Processings of the 1999 Joint International Meeting of Electrochemical Society*, Hawaii, (1999) 992.
6. N. Ravet, Y. Chouinard, J.F. Magnan, S. Besner, M. Gauthier, M. Armand, *J. Power Sources* 97–98 (2001) 503.
7. S.L. Bewlay, K. Konstantinov, G.X. Wang, S.X. Dou, H.K. Liu, *Mater. Lett.* 58(11) (2004) 1788.
8. M.M. Ren, Z. Zhou, X.P. Gao, W.X. Peng, *J. Phys. Chem. C* 112(14) (2008) 5689.
9. N. Meethong, Y.H. Kao, S.A. Speakman, Y.M. Chiang, *Adv. Funct. Mater.* 19(7) (2009) 1060.
10. K.W. Nam, W.S. Yoon, K. Zaghib, K.Y. Chung, X.Q. Yang, *Electrochem. Commun.* 11(10) (2009) 2023.
11. J. Zheng, X. Li, Z. Wang, S. Niu, D. Liu, *J. Power Sources* 195(9) (2010) 2935.
12. P. Gibot, M. Casas-Cabanas, L. Laffont, S. Levasseur, P. Carlach, S. Hamelet, J.M. Tarascon, C. Masquelier, *Nat. Mater.* 7(9) (2008) 741.
13. M. Gaberscek, R. Dominko, J. Jamnik, *Electrochem. Commun.* 9(12) (2007) 2778.
14. K. Saravanan, M.V. Reddy, P. Balaya, H. Gong, B.V.R. Chowdari, J.J. Vittal, *J. Mater. Chem.*, 19 (2009) 605.
15. F. Cheng, W. Wan, Z. Tan, Y. Huang, H. Zhou, J. Chen, X. Zhang, *Electrochim. Acta* 56(8) (2011) 2999.
16. S. Beninati, L. Damen, M. Mastragostino, *J. Power Sources* 194(2) (2009) 1094.
17. J. Chen, M.S. Whittingham, *Electrochem. Commun.* 8 (5) (2006) 855.
18. M. Higuchi, K. Katayama, Y. Azuma, M. Yukawa, M. Suhara, *J. Power Sources* 119–121(2003) 258.

19. C. Sun, S. Rajasekhara, J.B. Goodenough, F. Zhou, *J. Am. Chem. Soc.* 133 (2011) 2132.
20. J.K. Kim, G. Cheruvally, J.W. Choi, J.U. Kim, J.H. Ahn, G.B. Cho, K.W. Kim, H.J. Ahn, *J. Power Sources* 166(1) (2007) 211.
21. H.C. Shin, W.I. Cho, H. Jang H., *J. Power Sources* 159(2) (2006) 1383.
22. G. Arnold, J. Garche, R. Hemmer, S. Strobele, C. Vogler, M. Wohlfahrt-Mehrens, *J. Power Sources* 119-121(2003) 247.
23. Y. Ding, Y. Jiang, F. Xu, J. Yin, H. Ren, Q. Zhuo, Z. Long, P. Zhang, *Electrochem. Commun.* 12(1) (2010) 10.
24. S.Y. Lim, C.S. Yoon, J. P.Cho, *Chem. Mater.* 20(14) (2008) 4560.
25. H. Liu, C. Li, H.P. Zhang, L.J. Fu, Y.P. Wu, H.Q. Wu, *J. Power Sources* 159(1) (2006) 717.
26. Y.Z. Dong, Y.M. Zhao, Y.H. Chen, Z.F. He, Q. Kuang, *Mater. Chem. Phys.* 115 (2009) 245.
27. H.J. Kim, J.M. Kim, W.S. Kim, H.J. Koo, D.S. Bae, H.S. Kim, *J. Alloys Compd.* 509(18) (2011) 5662.
28. Z. Xu, L. Xu, Q. Lai, X. Ji, *Mater. Res. Bull.* 42(5) (2007) 883.